Contribution to Substrate Specificity and Transport of Nonconserved Residues in Transmembrane Domain 12 of Human P-Glycoprotein †

ARTICLE *in* BIOCHEMISTRY · DECEMBER 1998

Impact Factor: 3.02 · DOI: 10.1021/bi980871+ · Source: PubMed

6 AUTHORS, INCLUDING:

Peter Hafkemeyer
Universitätsklinikum Freiburg
32 PUBLICATIONS **623** CITATIONS
SEE PROFILE

Suresh V Ambudkar
National Institutes of Health
258 PUBLICATIONS **14,473** CITATIONS
SEE PROFILE

Contribution to Substrate Specificity and Transport of Nonconserved Residues in Transmembrane Domain 12 of Human P-Glycoprotein†

Peter Hafkemeyer,‡ Saibal Dey,‡ Suresh V. Ambudkar,‡ Christine A. Hrycyna,‡ Ira Pastan,§ and Michael M. Gottesman*,‡

Laboratories of Cell Biology and of Molecular Biology, Division of Basic Sciences, National Cancer Institute, National Institutes of Health, Bethesda, Maryland 20892

Received April 17, 1998; Revised Manuscript Received August 18, 1998

ABSTRACT: P-glycoprotein (Pgp), the product of the *MDR*1 gene, confers multidrug resistance on cancer cells by ATP-dependent extrusion of anticancer drugs. Biochemical and genetic studies with Pgp have identified the putative transmembrane (TM) region 12 (residues 974−994) as a major region involved in drug interactions with amino acid residues conserved among Pgp family members shown to be essential for transport. To determine whether nonconserved residues might be involved in substrate specificity, seven amino acid residues were identified within TM 12 that were not strictly conserved among the *MDR*1 and *MDR*2 family of proteins from different mammalian species. We replaced all seven of these amino acid residues with alanine, one at a time and in combinations, and used a vaccinia virus based transient expression system to analyze function. None of the single replacements caused any alteration in transport function. However, when residues L975, V981, and F983 were replaced collectively, drug transport, drug-stimulated ATP hydrolysis, and photoaffinity labeling with the drug analogue, [^{125}I]iodoarylazidoprazosin (IAAP), were abrogated, with little effect on [α-^{32}P]-8-azido-ATP labeling and basal ATPase activity. Pairwise alanine substitutuions showed variable effects on function. Substitutions including L975A in combination with any one of the other two replacements had the least effect on Pgp function. The V981A and F983A double mutant showed the most effect on transport of fluorescent substrates. In contrast, alanine substitutions of all four nonconserved residues M986, V988, Q990, and V991 at the putative carboxy-terminal half of TM 12 showed no effect on drug transport except for a partial reduction in bodipy-verapamil extrusion. These results suggest that nonconserved residues in the putative amino-proximal half of TM 12 of Pgp play a more direct role in determining specificity of drug transport function than those in the putative carboxy-terminal half of TM 12.

The human multidrug transporter (P-glycoprotein, or Pgp) encoded by the *MDR*1 gene, is a 1280 amino acid integral membrane phosphoglycoprotein that functions as an ATP-dependent efflux pump for structurally diverse anticancer drugs as well as cytotoxic compounds (*1, 2*). Expression of *MDR*1 in cancer cells confers resistance to multiple chemotherapeutic agents. To overcome *MDR*1-mediated drug resistance, its mechanism of action has to be properly understood. In the absence of direct structural information, this analysis has relied exclusively on genetic and biochemical characterization of the transporter. Single amino acid replacement and domain swapping experiments have identified important regions within Pgp that are either directly or indirectly involved in drug transport (*2*−*5*).

Photoaffinity labeling with substrate analogues has identified regions in and around TM 5 and 6 as well as TM 11 and 12 as the major drug interaction sites of Pgp (*6*−*8*). Mutational analysis has shown that among the 12 TM regions in Pgp, TM 5 and 6 in the N-terminal half and TM 11 and 12 in the C-terminal half play an active role in drug transport and substrate specificity (9 and 10). Sequence alignment of these four TM domains (5, 6, 11, and 12) from homologous transporters suggests a high degree of homology among the members of the *MDR*1 and *MDR*2 (phosphatidylcholine transporter) families from different species. Replacement of the conserved residues (for example, F978A) within the TM regions has profound effects on the substrate specificity and transport function of Pgp (*11*).

Characterization of human MDR1/MDR2 chimeric proteins demonstrates that replacement of TM 12 of human MDR1 with TM 12 of human MDR2 results in loss of function as a drug transporter (*4*). Sequence alignment of TM 12 detected seven amino acid residues that were not strictly conserved among the members of the *MDR*1 and *MDR*2 family. Because these residues may be responsible for the differences in substrate specificity of *MDR*1 and *MDR*2, we characterized the role of these nonconserved amino acid residues in TM 12 in drug transport and substrate specificity. All seven residues were changed to alanines, either one at a time or in groups. Using an efficient vaccinia-

† Peter Hafkemeyer is the recipient of a grant from the Deutsche Forschungsgemeinschaft (DFG), Germany.

* Corresponding author: Michael M. Gottesman, M. D., Laboratory of Cell Biology, Bldg 37; Room 1A09, National Cancer Institute, National Institutes of Health, 37 Convent Dr. MSC4255, Bethesda, MD 20892-4255. Telephone: (301)-496-1530. Fax: (301) 402-0450. E-mail: mgottesman@nih.gov.

‡ Laboratory of Cell Biology.

§ Laboratory of Molecular Biology.

10.1021/bi980871+
Published on Web 10/26/1998

based transient expression system suitable for analysis of mutant Pgp's, we have characterized 12 individual mutants. Our results provide evidence that nonconserved amino acid residues in the putative amino-proximal half of the TM 12 of MDR1 collectively play a role in determining substrate specificity and drug transport.

MATERIALS AND METHODS

Materials. Minimum essential medium with Earle's salts (EMEM), Opti-MEM, Iscove's modified Dulbecco's medium (IMEM), trypsin-EDTA, and lipofectin were obtained from Gibco (Gaithersburg, MD). Fetal bovine serum (FBS) was from HyClone Laboratories (Logan, UT). Dulbecco's modified Eagle's medium (DMEM) without glutamine was obtained from Quality Biological Inc. (Gaithersburg, MD). [^{125}I]Iodoarylazidoprazosin (IAAP, 2200 Ci/nmol; 1 Ci = 37 GBq) was purchased from DuPont NEN (Boston, MA) and [α-^{32}P]-8-azido-ATP (specific activity 23 Ci/mmol; 2 mCi/mL) from ICN (Irvine, CA). Calcein-AM, Rhodamine 123, bodipy-verapamil and bodipy-taxol were obtained from Molecular Probes, Inc. (Eugene, OR). Daunorubicin and cyclosporin A were obtained from Calbiochem (San Diego, CA). Restriction enzymes were from Boehringer Mannheim (Indianapolis, IN) and New England Biolabs (Beverly, MA).

Cell Lines and Viruses. Human osteosarcoma cells (HOS, ATCC CRL1543) and HeLa cells were grown as described previously by Ramachandra et al. (*12*) and Hrycyna et al. (*13*). Recombinant vaccinia virus encoding bacteriophage T7 RNA polymerase (vTF7-3) (ATCC VR2153) was propagated and purified as described (*14*).

Mutagenesis and Vector Construction. In TM 12 of human P-glycoprotein alanine mutations were constructed using the pTM1 MDR1 vector system (*12*). In this system the human MDR1 cDNA sequence is inserted at the 3′ end of the encephalo-myocarditis virus internal ribosome entry site (IRES) sequence downstream from the T7 promoter in pTM (*15, 16*). Alanine mutations were introduced using a PCR mutagenesis method (*17*) at positions L975, V981, F983, M986, V988, Q990, and V991. In addition to those single mutations a triple alanine mutant encompassing L975, V981, and F983 and a quadruple alanine mutant encompassing M986, V988, Q990, and V991 were constructed. Moreover, double mutants based on the triple mutant were cloned (L975A-V981A-F983, L975A-V981-F983A, L975-V981A-F983A). PCR fragments containing the respective mutations spanned the unique NdeI and PstI sites (625 base pairs) in the human MDR1 cDNA and were subsequently cloned into these sites. All Nde I−Pst I mutant fragments were sequenced in their entirety in both directions including the insertion points and flanking regions by automated sequencing (PRISM Ready Reaction DyeDeoxy Terminator Sequencing Kit, Perkin-Elmer Corp., Norwalk, CT).

Expression of P-Glycoprotein by Infection−Transfection. The vaccinia-based transient expression system used was based on the method developed by Moss and colleagues (*16, 18*). The transfection−infection procedure was performed as described previously by Ramachandra et al. (*12*) and Hrycyna et al. (*13*).

Fluorescence Activated Cell Sorting (FACS). Cell surface expression of wild-type and mutant P-glycoproteins was detected essentially as previously described by Ramachandra et al. (*12*) and Hrycyna et al. (*13*) using 5×10^5 cells and either 5 μg human Pgp specific MRK16 antibody or 5 μg purified mouse IgG1a, keppa anti- TNP as an isotype control (Pharmingen, San Diego, CA). Incubation was for at least 30 min on ice. Afterward the cells were carefully washed twice with IMEM supplemented with 5% FBS. The cells were then incubated for another 30 min to 1 h with 3 μg FITC-labeled anti-mouse IgG2a, washed, then resuspended in 350 μL of cold PBS and analyzed by Fluorescence Activated Cell Sorting FACS) (Becton-Dickinson FACS System, equipped with the CellQuest program, San Jose, CA). The results are presented as cell number versus intracellular fluorescence intensity.

For fluorescent drug accumulation assays, 5×10^5 cells were incubated in 5 mL of IMEM containing 5% FBS and final concentrations of either 0.5 μg/ml rhodamine 123, 0.5 μM bodipy-verapamil, 0.1 μM bodipy-taxol, and 0.5 μM calcein-AM or 4 μM daunorubicin with or without 5 μM cyclosporin A as reversing agent. Incubation was for 10 min for calcein-AM accumulation, 30 min for 0.5 μM bodipy-verapamil and 0.1 μM bodipy-taxol accumulation, and 40 min for rhodamine 123 and daunorubicin accumulation at 37 °C. For rhodamine 123 and daunorubicin measurements, cells were resuspended and incubated for another 40 min at 37 °C in the presence and absence of 5 μM cyclosporin A. Cells were then resuspended in cold PBS and analyzed by FACS. The results are presented as cell number versus intracellular fluorescence intensity.

Preparation of Crude HeLa Membranes. Crude membranes from vaccinia virus infected HeLa cells were prepared as described previously by Ramachandra et al. (*12*). Briefly, cells were washed twice in phosphate buffered saline (PBS) containing 1% aprotinin and incubated on ice for 45 min in 7 mL of lysis buffer [10 mM Tris-HCl pH 7.5, 10 mM NaCl, 1 mM $MgCl_2$, 1 mM DTT, 1% aprotinin, 1 mM 4-(2-aminoethyl)benzenesulfonyl fluoride (AEBSF) (ICN, CA)] and disrupted with a Dounce homogenizer. Following lysis, undisrupted cells and nuclei were removed by centrifugation at 500*g* for 10 min. Microccocal nuclease was added to the supernatant to a final concentration of 5 U/mL and $CaCl_2$ to a final concentration of 1 mM. After incubation on ice for 20 min, the supernatant was centrifuged at 100000*g* for 30 min at 4 °C. The pellet was resuspended in 400 μL resuspension buffer (10 mM Tris-HCl pH 7.5, 50 mM NaCl, 250 mM sucrose, 1mM DTT, 1% Aprotinin, 1mM AEBSF) containing 10% glycerol by passing through a hypodermic needle (gauge size 23) and stored at −70 °C.

SDS−PAGE and Immunoblot Analysis. Electrophoresis and immunoblot analysis were performed as described previously (*19*).

Photoaffinity Labeling with Substrate Analogue. Photoaffinity labeling was carried out according to Bruggemann et al. (*8*), with slight modifications. A total of 50 μg of crude membranes were diluted to 98 μL with 50 mM Tris-HCl pH 7.5 and either 1 μL of DMSO or 1 μL of a cyclosporin A stock solution (0.5 mM) for binding competition and 1 μL of IAAP (3−4 nM) and incubated for 10 min under subdued light. Following incubation, membranes were illuminated with a UV lamp (General Electric no. F15T8-BLB; 366 nm) for 10 min, in water, at room temperature.

Photoaffinity Labeling with [α-^{32}P]-8-Azido-ATP. [α-^{32}P]-8-azido-ATP labeling was done with 50 μg of crude

membranes in 10 mM Tris-HCl pH 7.5, 50 mM NaCl, 250 mM sucrose, 10 mM $MgCl_2$, 1% aprotinin (Sigma, MO) and 0.3 mM AEBSF. Membranes were incubated for 3 min on ice before addition of 2.5 μM [α-^{32}P]-8-azido-ATP under subdued light. Following addition, membranes were incubated for another 10 min on ice in the dark. Afterward UV-cross-linking was performed at 366 nm for 20 min on ice.

Vanadate-induced [α-^{32}P]-8-azido-ADP trapping was performed in the presence and absence of 0.3 mM vanadate with the same buffer conditions described above. Preincubation with or without vanadate was done for 5 min at 37 °C. [α-^{32}P]-8-azido-ATP and nonradioactive 8-azido-ATP was added so to have a final concentration of 10 μM cold 8-azido-ATP and 6 μCi [α-^{32}P]-8-azido-ATP per sample. Incubation was for 10 min at 37 °C in the dark and then for 5 min on ice. UV cross-linking was performed at 366 nm for 10 min on ice.

All samples were immunoprecipitated with 600 μL of RIPA buffer (20 mM Tris-HCl, pH 7.5, 150 mM NaCl, 1% (v:v) Triton X-100, 1% (w:v) sodium deoxycholate, 0.1% (w:v) sodium dodecyl sulfate, 1 mM ethylenediaminetetraacetic acid (EDTA)) and 6 μL of anti-Pgp polyclonal antibody PEPG 2 (20). Samples were incubated for 2 h at 4 °C on a rotary shaker and then 40 μl Protein A agarose (Gibco, Gaithersburg, MD) was added. Incubation was for another 2 h at 4 °C. The beads were washed 3 times with RIPA buffer and then eluted with 80 μL of 1.5 × SDS−PAGE loading buffer for 30 min at room temperature. The samples were then subjected to SDS−PAGE.

Measurement of ATPase Activity. Pgp-associated ATPase activity was measured by determining the vanadate-sensitive release of inorganic phosphate from ATP in the presence and absence of verapamil with a colorimetric method as described by Sarkadi et al. (*21*).

RESULTS

Sequence Alignment of TM 12 of Various Multidrug Tansporters and Alanine Scanning. To determine which residues were nonconserved among the *MDR*1 and *MDR*2 genes, we aligned the amino acid sequences of mouse *mdr* 1a, *mdr* 1b, *mdr* 2, hamster *pgp* 1, *pgp* 2, *pgp* 3, rat *mdr*1, *mdr*2, and human *MDR*1 and *MDR*2. Amino acid residues L975, V981, F983, M986, V988, Q990, and V991 in human *MDR*1were found not to be strictly conserved (Figure 1a). The previous study by Zhang et al. (*4*) in which the TM 12 segment from *MDR*2 was substituted for *MDR*1 TM 12 replaced these residues with *MDR*2-like residues. Therefore, it was not clear whether the loss of *MDR*1 transport function shown in this previous study was due to the loss of the *MDR*1 residues or due to the substitution with *MDR*2 residues. To differentiate between these two possibilities, the nonconserved residues were changed to alanine one at time and also in combination. Alanine was chosen as a replacement, since it is a small neutral amino acid that would preserve any possible α-helical nature of the transmembrane segment as well as minimize alterations in the structural integrity of the protein. Alanine mutants were arranged in such a way that three alanine mutations were putatively located in the outer plasma membrane leaflet (L975A, V981A, and F983A) and four in the inner leaflet (M986A, V988A, Q990A, and V991A), assuming an α-helical structure to TM 12 (Figure 1b).

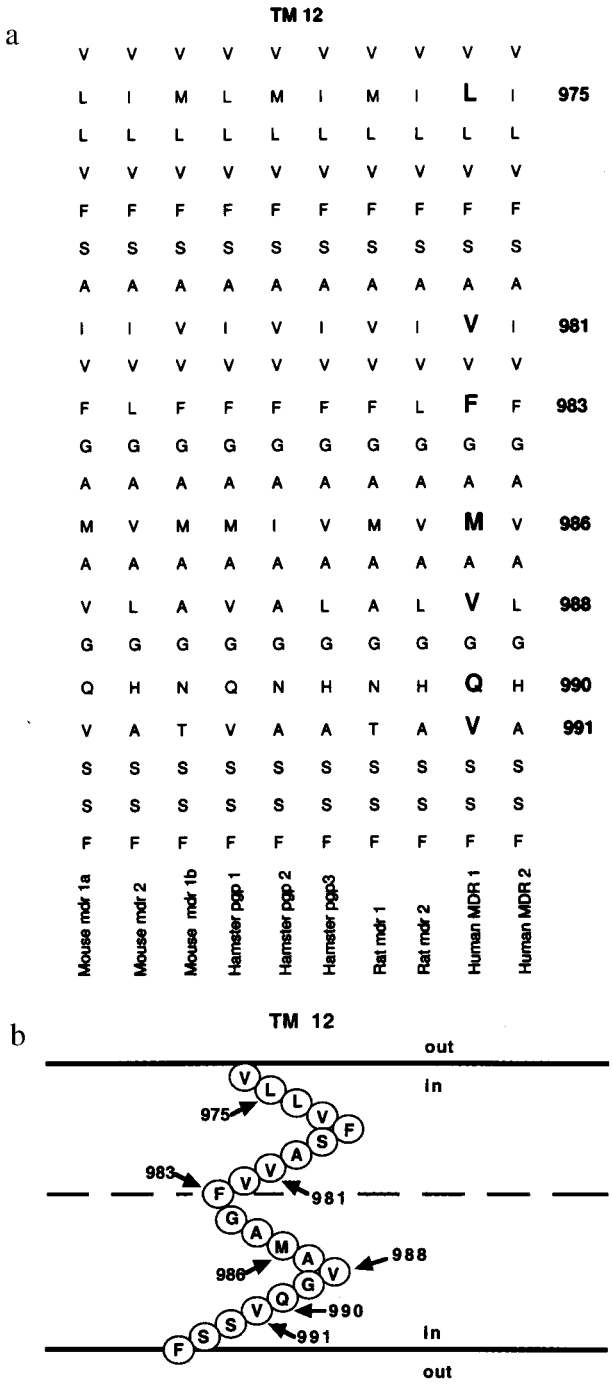

FIGURE 1: Panel a: Amino acid sequence alignment of the putative transmembrane domain 12 (amino acids 974 to 994) of mammalian P-glycoproteins. The residues in bold letters represent the nonconserved amino acid residues within the Pgp family from mouse, hamster, rat and human that were studied in this work. Panel b: Schematic drawing shows possible positions of these residues in TM 12.

Cell Surface Expression of Wild-Type and Mutant P-Glycoproteins. Wild-type or mutant *MDR*1 cDNAs were cloned into a vaccinia expression vector (pTM1) downstream from a T7 promoter and transfected into human osteosarcoma cells (HOS). High level expression of Pgp can be obtained after transfection of this vector after infection with a recombinant vaccinia virus that encodes the gene for T7 polymerase. To compare the amount of Pgp expressed by cells transfected with wild-type or mutant genes, the transfected cells were analyzed by FACS using the monoclonal

Table 1: Properties of Wild-Type and Mutant P-glycoproteins[a]

	drug transport[a]					
	cell surface expression[c]	rhodamine	daunomycin	bodipy-verapamil	calcein-AM	bodipy-taxol
wild-type	++++	++++	++++	++++	++++	++++
L975A	++++	++++	++++	++++	++++	++++
V981A	++++	++++	++++	++++	++++	++++
F983A	++++	++++	++++	++++	++++	++++
M986A	++++	++++	n.d.	++++	++++	n.d.
V988A	++++	++++	n.d.	++++	++++	n.d.
Q990A	++++	++++	n.d.	++++	++++	n.d.
V991A	++++	++++	n.d.	++++	++++	n.d.
L975A, V981A, F983A	++++	no transport	no transport	++	++	++
M986A, V988A, Q990A, V991A	++++	++++	+++	++	++++	++++
V981A, F983A	++++	+	no transport	++	++	+++
L975A, F983A	++++	+	++	++++	+++	++++
L975A, V981A	++++	++	no transport	++++	+++	++++

[a] Symbols are noted as follows: ++++, wild-type activity; ++, impaired activity; +, residual activity; and n.d., not determined. [b] Drug transport was determined by FACS. [c] Cell surface expression of wild-type and mutant Pgp's was determined by fluorescence activating cell sorting using the monoclonal antibody MRK 16.

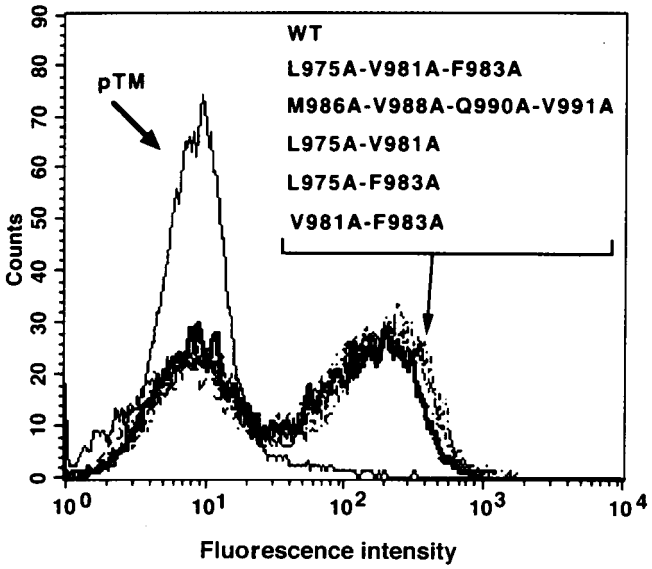

FIGURE 2: Cell surface expression of wild-type (WT) and mutant Pgp's using the monoclonal antibody MRK-16. pTM (cells infected with vTF 7-3 virus and transfected with the expression vector containing no MDR1 (pTM1) (negative control, —), WT (wild-type human MDR1, —). Mutant Pgp's are the triple mutant in the amino-proximal half of TM 12 (L975A—V981A—F983A, — —), the quadruple mutant in the carboxy-terminal half of TM 12 (M986A—V988A—Q990A—V991A, ···), the double mutants L975A—V981A (- - -), L975A—F983A (-··-), and V981A—F983A (—·—).

antibody MRK-16. All of the mutant Pgp's investigated were expressed on the cell surface at approximately wild-type Pgp level (Figure 2 and Table 1). By using this system, a transfection efficiency of 50% was routinely achieved. Cells transfected with wild-type *MDR*1 served as the positive control in this system and cells transfected with the expression vector pTM1, without the *MDR*1 cDNA insert, as a negative control.

Drug Transport Properties of Wild-Type and Mutant P-Glycoproteins by FACS Analysis Using Fluorescent Substrates. Analyzing the MDR1 transport activity was done by fluorogenic substrate accumulation assays. Fluorogenic substrates accumulated in cells lacking functional Pgp. Cells expressing high Pgp activity accumulate less substrate and are therefore less fluorescent. We used calcein-AM, bodipy-verapamil, rhodamine 123, bodipy-taxol, and daunorubicin as substrates. Cyclosporin A served as an inhibitor of Pgp-mediated drug transport. Drug transport activities for wild-type Pgp and all Pgp mutants were determined in the presence and absence of 5 μM of cyclosporin A. Drug transport was completely inhibited in the presence of cyclosporin A. Wild-type Pgp was able to extrude the fluorogenic substrates used in this study and therefore those cells had the lowest fluorescence intensity compared to cells transfected with the expression vector alone (pTM1 expressing no Pgp).

FACS analysis using fluorescent substrates of the single nonconserved alanine mutants showed that none of them alone significantly altered the drug transport profiles of Pgp's compared to wild-type MDR1 (Table 1), suggesting that none of these nonconserved amino acid residues alone are essential for interaction with Pgp.

In contrast, no transport of rhodamine 123 and daunorubicin was detectable when all three amino acid residues in the amino-proximal half of transmembrane domain 12 (L975, V981, and F983) were substituted with alanines. These cell populations contained the same fluorescence intensity as the negative control pTM1. Transport of bodipy-verapamil, bodipy-taxol, and calcein-AM was also significantly reduced (lower fluorescence intensity compared to wild-type Pgp), but not eliminated (Figure 3).

Substitution of the four nonconserved amino acid residues (M986A, V988A, Q990A, and V991A) in the carboxy-terminal half of TM 12 had no effect on transport of calcein-AM, rhodamine 123, and bodipy-taxol. Bodipy-verapamil and daunorubicin transport were only partially reduced. These findings suggest that changes in the amino-proximal half of TM 12 are more crucial than in the carboxy-terminal half of TM 12 of human *MDR*1 (Figure 3), and we therefore did not further investigate any combinatorial changes in the four nonconserved residues in the carboxy-terminus of TM 12.

Double mutants combining pairwise L975A, V981A, and F983A were constructed in order to determine the critical nonconserved residues that were responsible for mediating drug transport in the amino-proximal half of TM 12. Those double mutants were L975A—V981A, L975A—F983A, and V981A—F983A. The V981—F983 double mutant was

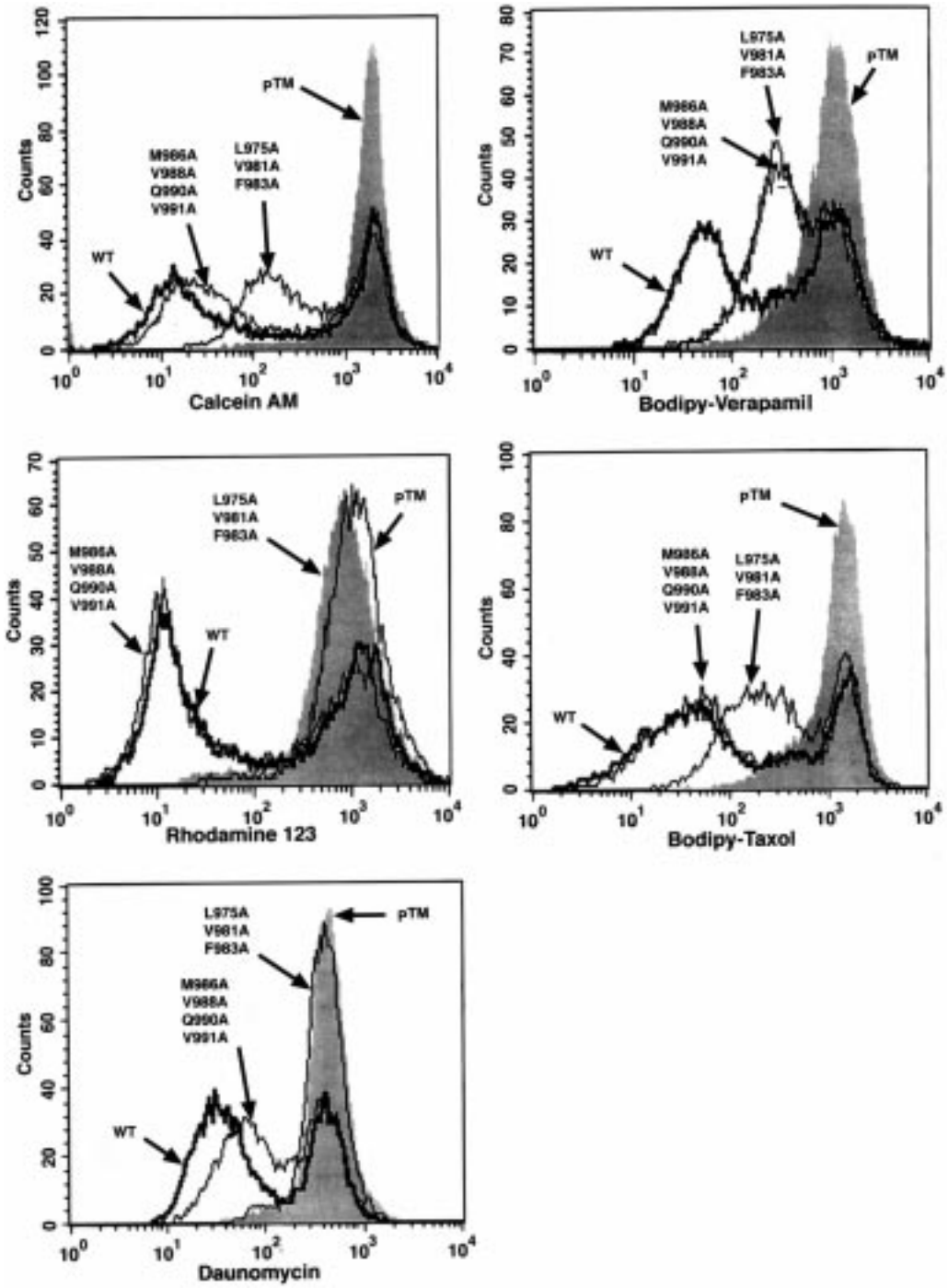

FIGURE 3: Determination of transport of fluorescent substrates including calcein AM, bodipy verapamil, rhodamine 123, bodipy-taxol, and daunorubicin as described in Material and Methods. Transport activities were determined for wild-type (WT) and mutant Pgp's. pTM (cells infected with vTF 7-3 virus and transfected with the expression vector containing no MDR1 (pTM1) (negative control, gray shaded area), WT (wild-type human MDR1, —). Mutant Pgp's are the triple mutant in the amino-proximal half of TM 12 (L975A−V981A−F983A) and the quadruple mutant (M986A−V988A−Q990A−V991A) (—).

impaired for transport of the substrates calcein-AM, bodipy-verapamil, and bodipy-taxol. Almost no transport function was detectable for rhodamine 123 and daunorubicin. This phenotype is virtually indistinguishable from that of the triple mutant (see Table 1). The double mutants involving L975A and either V981A and/or F983A were still capable of transporting calcein-AM, bodipy-taxol, and bodipy-verapamil but rhodamine 123 and daunorubicin transport was significantly reduced compared to wild-type Pgp (Figure 4), indicating a significant contribution of L975 to drug specificity.

These results implied that both V981 and F983 are most critically involved in drug transport of bodipy-taxol, bodipy-verapamil, and calcein-AM. Furthermore alteration in any two of the three nonconserved amino acid residues abrogates the ability of Pgp to transport daunorubicin and rhodamine 123.

Photoaffinity Labeling of Wild-Type and Alanine Mutant P-Glycoproteins. To determine the ability and specificity of the mutant Pgp's to bind substrates we used [^{125}I]-iodoarylazidoprazosin (IAAP), a photoactive analogue of prazosin. Immunoblotting with the monoclonal antibody

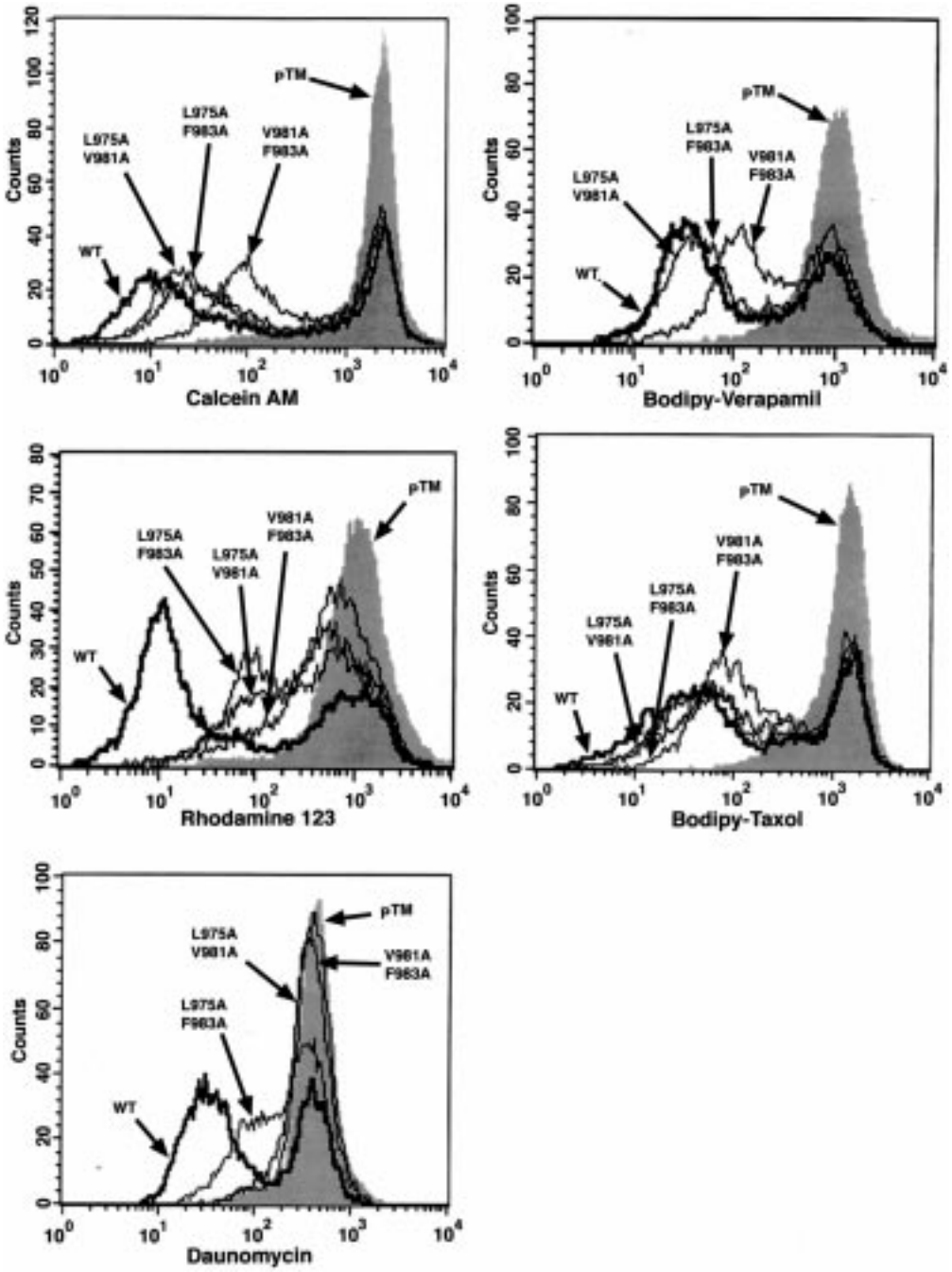

FIGURE 4: Determination of accumulation of calcein AM, bodipy-verapamil, rhodamine 123, bodipy-taxol, and daunorubicin. Accumulation was determined for wild-type (WT) and mutant Pgp's. pTM (cells infected with vTF 7-3 virus and transfected with the expression vector containing no MDR1 (pTM1) (negative control, gray shaded area) WT (wild-type human MDR1, −). Mutant MDR1s are double mutants L975A−V981A, L975A−F983A, and V981A−F983A (−).

C219 in these experiments showed the expression of wild-type and mutant Pgp's was comparable, but not identical in these experiments (Figure 5a). IAAP binding was specific for mutant Pgp's since IAAP binding could be competed with the MDR1 inhibitor cyclosporin A to the same extent as observed for wild-type Pgp (Figure 5b).

Photoaffinity labeling demonstrated that the triple mutant L975A−V981A−F983A displayed a significant reduction in binding of IAAP compared to wild-type Pgp which is consistent with its reduced drug transport ability (Figure 5b). The quantification of IAAP binding was done after normalization to Pgp expression levels (Figure 5c) as determined by Western blots (Figure 5a). The quadruple mutant, M986A−V988A−Q990A−V991A, in the carboxy-terminal half still retained a substantial ability to bind IAAP. The three double mutants L975A−V981A, L975A−F983A, and V981A−F983A were able to bind IAAP but somewhat less than wild-type Pgp as was also true for the single mutants investigated in this study (Figure 5b,c).

ATP hydrolysis by Alanine Mutants. To evaluate the influence of altered drug binding on substrate-stimulated ATPase activity and therefore on drug transport properties we measured the vanadate-sensitive verapamil-stimulated release of inorganic phosphate from Mg-ATP (Figure 6a,b). In the presence of 20 μM verapamil, we observed approximately 2−4-fold stimulation of wild-type MDR1 ATPase activity (Figure 6a,b). The triple mutant in the amino-terminal half of TM 12 showed less ATPase stimulation

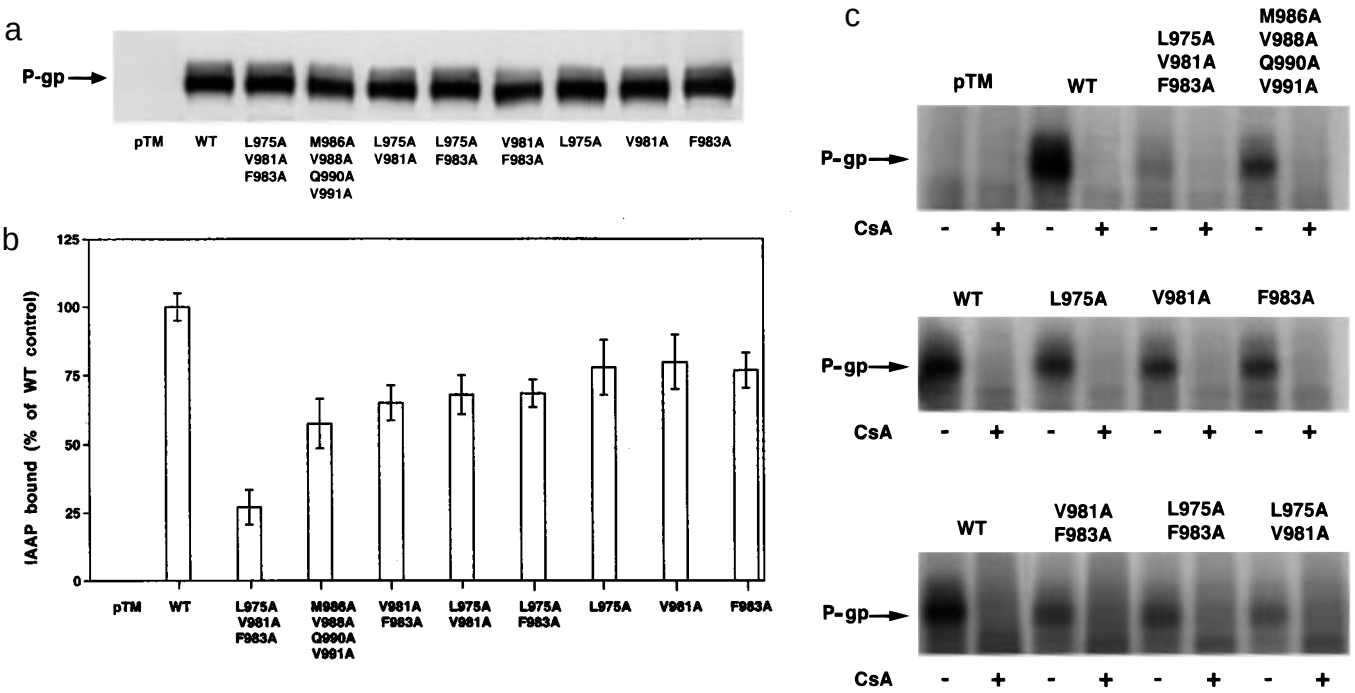

FIGURE 5: Photoaffinity labeling of wild-type and mutant Pgp's. (a) Quantification of wild-type and mutant Pgp's in crude membranes by immunoblotting. 5 μg of HeLa crude membranes were applied to SDS-PAGE (8%) detected with the polyclonal antibody C219. Photoaffinity labeling of wild-type and mutant Pgp's with [^{125}I]IAAP in the presence and absence of cyclosporin A; (b) Effect of cyclosporin A on [^{125}I]IAAP labeling of wild-type (WT) and mutant Pgp's. Photoaffinity labeling of 20 μg of Pgp containing crude HeLa cell membranes was carried out with 5 nM of [^{125}I]IAAP in the presence or absence of 5 μM cyclosporine A. After UV-crosslinking, Pgp's were separated on a 8% gel by SDS−PAGE and subjected to autoradiography. (c) Quantification of IAAP binding was done with a STORM 860 phosphoimaging system (Molecular Dynamics) after normalizing the expression of wild-type and mutant Pgp's by immunoblotting. The means from three independent experiments are given with the corresponding standard error.

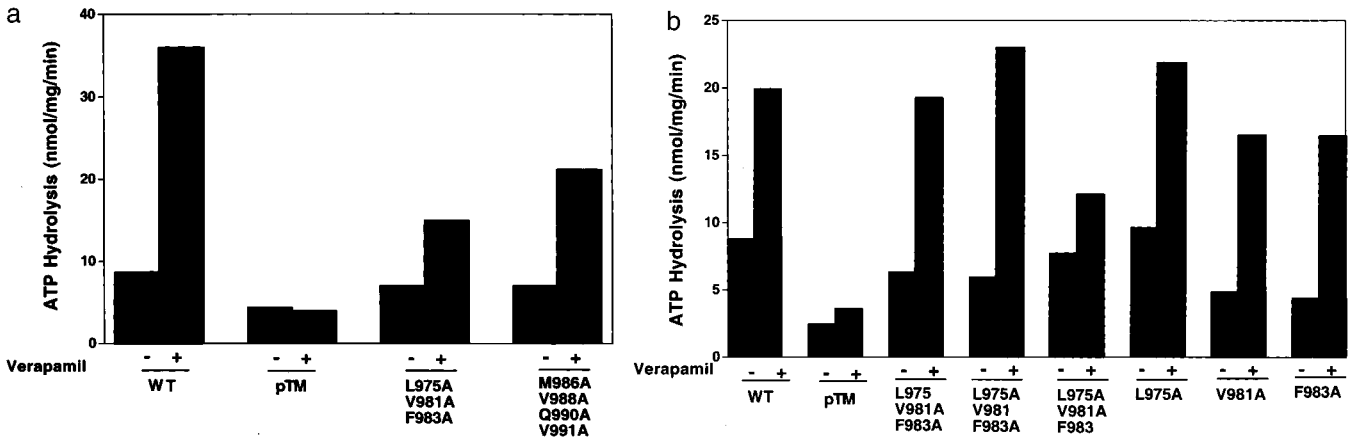

FIGURE 6: Verapamil-stimulated ATP hydrolysis of wild-type and mutant Pgp's in 20 μg of crude membranes from infected−transfected HeLa cells. The vanadate-sensitive activities calculated as the differences between the ATPase activities measured in the absence and presence of vanadate (300 μM) are plotted. Verapamil-stimulated ATPase activity was determined in the presence of 25 μM verapamil. Representative data from two experiments are shown. (a) pTM: cells infected with vTF 7-3 virus and transfected with the expression vector containing no MDR1 (pTM1) (negative control), WT (wild-type human MDR1), and mutant Pgp's are the triple mutant in the amino-proximal half of TM 12 (L975A−V981A−F983A) and the quadruple mutant in the carboxy-terminal half of TM 12 (M986A−V988A−Q990A−V991A). (b) pTM: cells infected with vTF 7-3 virus and transfected with the expression vector containing no MDR1 (pTM1) (negative control), WT (wild-type human MDR1). Mutant MDR1s are the three double mutants L975A−V981A, L975A−F983A, and V981A−F983A.

compared to wild-type in the same experiment (Figure 6a). In contrast, the quadruple mutant in the carboxy-terminal half of TM 12 displayed approximately 3-fold verapamil-stimulated ATPase activity. The double and single mutants displayed near wild-type levels of verapamil-stimulated ATPase activity except for L975A−V981A (Figure 6b).

ATP Binding and Vanadate Trapping of Alanine Mutants. To confirm that reduction in ATP hydrolysis of the triple and respective double mutants was not due to impaired ATP binding, we performed [α-^{32}P]-8-azido-ATP labeling (Figure 7). ATP binding was equivalent for wild-type MDR1 and the MDR1 mutants L975A−V981A−F983A as well as for M986A−V988A−Q990A−V991A (Figure 7). Senior's group previously showed that in the presence of vanadate, [α-^{32}P]-8-azido-ATP is trapped in the ADP form (*22*). This requires ATP hydrolysis. Vanadate-trapped [α-^{32}P]-8-azido-ADP was significantly reduced in the triple mutant L975A−V981A−F983A (Figure 8b,c), consistent with the decrease

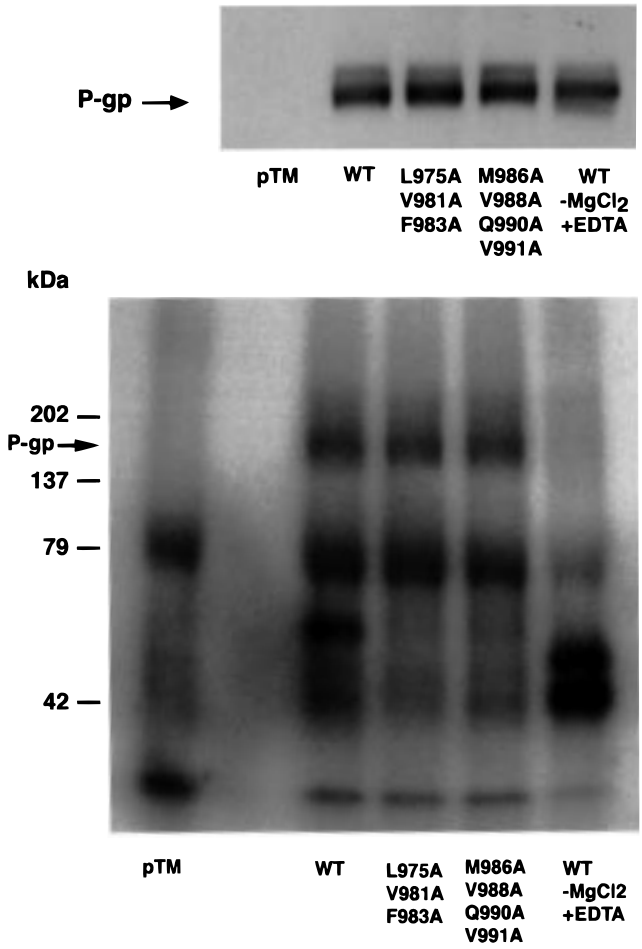

FIGURE 7: Binding of ATP to wild-type and mutant Pgp's. (Upper panel) Immunoblotting of wild-type and mutant Pgp's. 5 μg of HeLa crude membranes were applied to SDS−PAGE (8%) and detected with the polyclonal antibody C219. (Lower panel) [α-^{32}P]-8-Azido-ATP-binding of wild-type and mutant Pgp's. [α-^{32}P]-8-Azido-ATP-binding was performed using 50 μg of crude membranes from infected−transfected HeLa cells as described in Material and Methods. pTM: cells infected with vTF 7-3 virus and transfected with the expression vector containing no MDR1 (pTM1) (negative control), WT (wild-type human MDR1), the triple mutant in the amino-proximal half of TM 12 (L975A−V981A−F983A), the quadruple mutant in the carboxy-terminal half of TM 12 (M986A−V988A−Q990A−V991A), WT (wild-type human MDR1) in the presence of 250 μM EDTA and without $MgCl_2$ to assess the specificity of the 170 kDa band representing Pgp as indicated with the arrow.

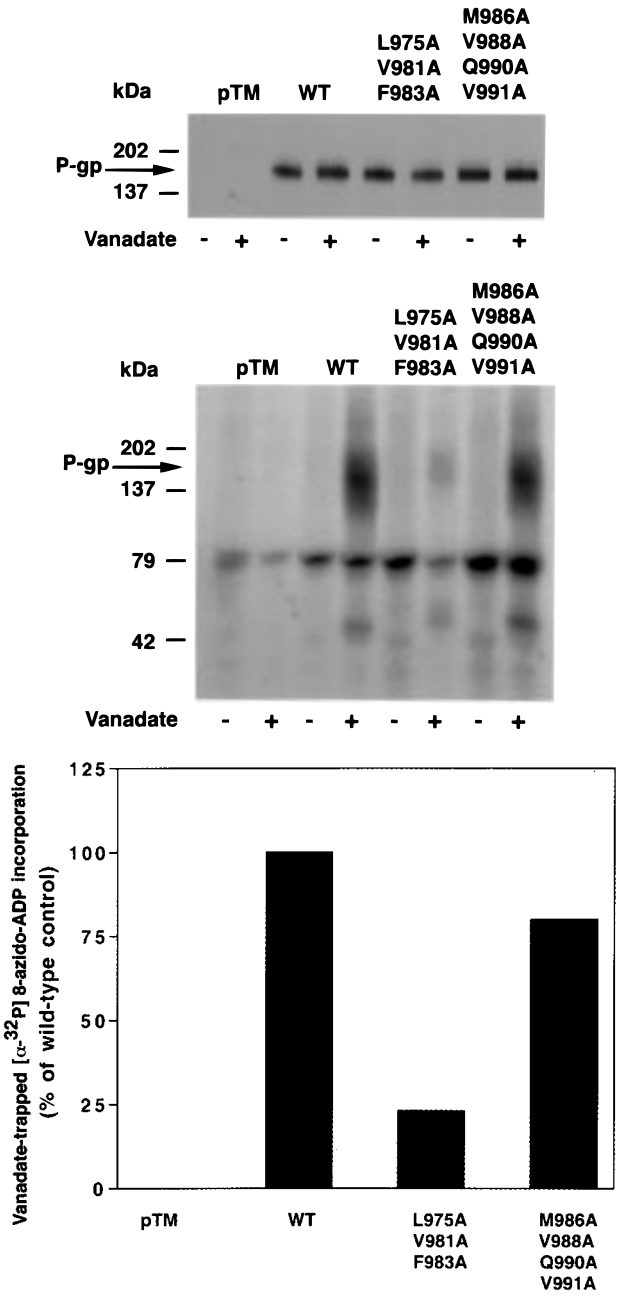

FIGURE 8: Vanadate-induced trapping of ADP to wild-type and mutant Pgp's. (Upper panel) Immunoblotting of wild-type and mutant Pgp's. 5 μg of HeLa crude membranes were applied to SDS−PAGE (8%) and detected with the polyclonal antibody C219. Vanadate-induced [α-^{32}P]-8-azido-ADP trapping. (Middle panel) Vanadate-induced [α-^{32}P]-8-azido-ADP labeling was performed at 37 °C. pTM: cells infected with vTF 7-3 virus and transfected with the expression vector containing no MDR1 (pTM1) (negative control), WT (wild-type human MDR1), the triple mutant in the amino-proximal half of TM 12 (L975A−V981A−F983A), and the quadruple mutant in the carboxy-terminal half of TM 12 (M986A−V988A−Q990A−V991A). (Lower panel) Quantification of ATP binding was done with a STORM 860 phosphoimaging system (Molecular Dynamics) after normalizing the expression of wild-type and mutant Pgp's by immunoblotting.

in the level of verapamil-stimulated ATPase activity noted above (Figure 6a). The quantification of vanadate-trapped [α-^{32}P]-8-azido-ADP was done after normalization to Pgp expression levels as assessed by immunoblotting (Figure 8a).

DISCUSSION

The multidrug transporter is known to have very broad substrate specificity. Identifying specific amino acid residues and domains involved in substrate recognition would contribute to understanding its mechanism of action, and may aid the molecular modeling of new cytotoxic drugs or modulators capable of blocking MDR1 function. The contribution of nonconserved amino acids to drug transport has not previously been investigated, even though they might be important determinants of differences in substrate specificity among Pgp family members. In this study we identified several residues in TM 12 of Pgp which are not completely conserved among known Pgp family members and show that although alanine substitutions of these specific residues do not abrogate Pgp function, substitution of combinations of these residues leads to loss of full activity and/or alterations in substrate specificity. This finding

supports the hypothesis that these nonconserved residues are involved in substrate recognition by *MDR*1. Of interest is that the predicted amino-proximal part of TM 12 of human *MDR*1 seems to be more crucially involved in drug transport.

Sequence Alignment of Transmembrane Region 12 of Different P-Glycoprotein Species. In this study we tried to identify amino acid residues in TM 12 that are necessary for substrate recognition by the multidrug transporter. We chose to make alanine substitutions, since alanine is a small neutral amino acid which should not interfere with the overall transmembrane structure. We focused on residues that were nonidentical among several known class I and class II MDR genes since the conserved residues have already been shown to be necessary for overall transport, but have not been shown to be sufficient to determine substrate specificity.

Previous alanine scanning experiments from Hanna et al. (*23)* in mouse *mdr*1b TM 11 demonstrated that the majority of mutants of conserved residues affect drug specificity, but leave the overall activity of Pgp intact. Loo and Clarke showed in their experiments that alanine mutants in human *MDR*1 TM 6 lacked the ability to confer drug resistance in transfected cells or conferred altered drug resistance (*24)*. Similarly, when TM 12 of human *MDR*1 was replaced by the homologous sequence of human *MDR*2 there was drastically reduced resistance to actinomycin D, vincristine, and doxorubicin (*4*). The use of chimeras has certain limitations compared to studying individual point mutations in that the relative importance of specific residues cannot be determined on the basis of comparative analysis of TM 12 among several different Pgp's. In this study, we identified seven amino acids in TM 12 which were not completely conserved among mouse, hamster, rat, and human class I and II MDRs. On the basis of a hypothetical model of TM 12 in the lipid bilayer (Figure 1), we divided those seven amino acids into two groups of which three are more amino-proximal (putative outer leaflet) and four are in the carboxy-terminus of TM 12 (putative inner leaflet).

Drug Transport Properties of Alanine Substitutions in TM 12 of Human Pgp. It is likely that alanine substitutions in TM 12 of human Pgp left the protein conformation intact so that proper folding could still occur since the monoclonal antibody MRK16 recognized these mutant proteins on the cell surface in amounts comparable to wild-type Pgp (Figure 2). It is still possible that the conformation in the mutants was locally affected, since MRK16 may not bind to epitopes that were mutated or affected by the mutations. As summarized in Tables 1 and 2, single amino acid changes to alanine had no significant effect on transport of the fluorescent substrates calcein-AM, rhodamine 123, bodipy-verapamil, bodipy-taxol, and daunomycin. Specificity of drug binding to these TM 12 mutants could be assessed by IAAP labeling in the absence and presence of 5 μM cyclosporin A (CsA), which affects binding of IAAP to both amino and carboxy halves of Pgp (*25*).

TM 6 mutations are known to affect interaction of CsA with Pgp *(26)*, consistent with a model in which both TM 12 and TM6 contribute to the CsA and IAAP interaction site(s). IAAP labeling appeared to be unchanged in these single mutants and verapamil-stimulated ATPase activity was at wild-type levels. These data suggest that these residues are not absolutely essential for Pgp function as a transporter, provided other residues remain intact.

Table 2: Properties of Wild-Type and Mutant P-Glycoproteins[a]

	photoaffinity labeling[a]	ATP binding[b]	ATPase activity[c]
wild-type	++++	++++	++++
L975A	+++	n.d.	+++
V981A	+++	n.d.	+++
F983A	+++	n.d.	+++
M986A	n.d.	n.d.	n.d.
V988A	n.d.	n.d.	n.d.
Q990A	n.d.	n.d.	n.d.
V991A	n.d.	n.d.	n.d.
L975A,V981A, F983A	+	++++	+
M986A, V988A, Q990A, V991A	++	++++	++
V981A, F983A	+++	n.d.	+++
L975A, F983A	+++	n.d.	+++
L975A, V981A	+++	n.d.	+++

[a] Symbols are noted as follows: ++++, wild-type activity; ++, impaired activity; +, residual activity; and n.d. not determined. [b] Photoaffinity labeling was done in HeLa crude membrane preparations using [^{125}I]iodoarylazidoprazosin. [c] ATP binding was done in HeLa crude membrane preparations using [α-^{32}P]-8-azido-ATP as described in Material and Methods. [d] Verapamil-stimulated vanadate sensitive ATP hydrolysis was measured in crude membranes of HeLa cells.

Changing all four amino acid residues M986A, V988A, Q990A, or V991A in the carboxy-terminal part of TM 12 still allows almost normal transport function of Pgp. The change of these four nonconserved amino acids has no effect on fluorescent drug transport, except for reduced bodipy-verapamil transport. This seems even more remarkable because this quadruple mutant results in a stretch of six amino acids out of which five are then alanines (see Figure 1b). ATP hydrolysis was still stimulated about 3-fold in the presence of verapamil, and vanadate trapping of [α-^{32}P]-8-azido-ADP was intact. Therefore, there seems to be a clear difference in contribution to drug transport between the amino-proximal and carboxy-terminal segments of TM 12. Although these residues are conserved among mouse *mdr*1b, hamster *pgp*1, and human *MDR*1, they do not seem to be essential for transport of the agents used in the study. Whether other substrates will be found to depend on these residues remains to be seen.

When all three nonconserved amino acid residues in the amino-proximal half of TM 12 were changed, drug transport was most dramatically affected for almost all drugs tested here, especially for rhodamine 123 and daunomycin. Moreover, a loss of verapamil-stimulated ATPase activity was observed leaving some basal ATPase activity intact. Consistent with the basal activity, ATP binding to this mutant protein was unaffected, which means that the integrity of the nucleotide binding domains was still preserved. IAAP labeling showed a significant reduction of interaction of this agent with Pgp and [α-^{32}P]-8-azido-ADP trapping was significantly reduced which is in accordance with the loss of drug-stimulated ATP hydrolysis. Therefore this mutant has impaired drug interaction, suggesting a collective role of the three amino acid residues in substrate recognition leading to reduced drug-stimulated ATPase activity.

To determine which combinations of these three residues of TM 12 predicted to lie in the outer leaflet were responsible for the loss of transport activity, we constructed double mutants (L975A−V981A, L975A−F983A, and V981A−F983A). The double mutants showed reduced drug transport suggesting that a change in any two of these three amino

acid residues renders the protein partially inactive. This is in sharp contrast to what we have found in the segment of TM 12 predicted to be in the inner leaflet, where little effect was observed even when all four residues were changed. In these double mutants drug binding as assessed by IAAP labeling was almost completely intact and so were the verapamil-stimulated ATPase activities. Therefore, no gross structural change has taken place in the double mutants and the degree of loss of transport function was dependent on the substrate used. This analysis suggests that amino acid residues 975, 981, and 983 contribute to the interaction of Pgp with substrates. While no single residue is crucial, combinations of residues, especially V981A and F983A, affect binding of specific substrates such as daunomycin and rhodamine 123. This result is consistent with biochemical studies showing at least two and possibly more binding sites for substrates to Pgp (*25*) and mutational analyses showing the effect of individual mutations on substrate specificity (*2*). Despite the high homology among mouse *mdr*1a, *mdr*1b, and human *MDR*1 there are distinct substrate preferences for each of them which can be attributed to nonconserved amino acids (*27*).

The differences in effect of substitutions of nonconserved amino acids in TM 12 in the predicted outer leaflet vs the inner leaflet has several possible implications. If the model is correct, this may imply that substrate interactions are predominantly in the outer leaflet, or that structural determinants which indirectly affect substrate binding are in this region of TM 12. Alternatively, it is possible that the model is incorrect and that the residues presumed to be in the inner leaflet are not in the membrane at all. In either case, this functional dissection of putative TM 12 has made it clear that certain regions of Pgp have more dramatic effects on substrate binding than other regions.

Of the three residues L975, was found to contribute relatively less to fluorescent drug transport than the others. Since mouse *mdr*1b, hamster *pgp*2, and rat *mdr*1 have a methionine (M) at this position and the class II Pgp's have an isoleucine (I) (Figure 1), this result could imply that this is a nonconserved residue that contributes relatively little to substrate specificity, but we have not tested all possible substrates. V981, which is among the two amino acid residues found to most affect fluorescent drug transport, is conserved among most members of the *MDR*1 family, except for mouse *mdr*1a and hamster *pgp*1 where it is an isoleucine (I). MDR homologues that are not multidrug transporters (human *MDR*2, mouse *mdr*2, hamster *pgp*3, and rat *mdr*2) have an isoleucine at this position. Therefore our finding that this valine residue in conjunction with other residues has an important role in transport of drugs such as daunomycin and rhodamine 123 is consistent with its relative conservation in *MDR*1 family members. F983A in combination with the other substitutions was also found to have a major effect on fluorescent drug transport. F983 is more completely conserved than the other two among the members of the *MDR*1 family and in only two instances (mouse *mdr*2 and rat *mdr*2) is it altered to leucine (L).

Taken together, our experimental results and the genetic and biochemical analyses of human Pgp suggest that drug recognition and transport by the multidrug transporter involves complex amino acid interactions with different conserved and nonconserved residues in TM 12 contributing to interaction with different substrates. Better understanding of the specific interactions will help in the design of compounds capable of overcoming drug resistance and therefore aid in anticancer chemotherapy.

REFERENCES

1. Gottesman, M. M., and Pastan, I. (1993) *Annu. Rev. Biochem. 62*, 385−427.
2. Gottesman, M. M., Hrycyna, C. A., Schoenlein, P. V., Germann, U. A., and Pastan, I. (1995) *Annu. Rev. Genet. 29*, 607−649.
3. Dhir, R., and Gros, P. (1992) *Biochemistry 31*, 6103−6110.
4. Zhang, X., Collins, K. I., and Greenberger, L. M. (1995) *J. Biol. Chem. 270*, 5541−5448.
5. Choi, K., Chen, C., Kriegler, M., and Roninson, I. B. (1986) *Cell 47*, 381−389.
6. Morris, D. I., Greenberger, L. M., Bruggemann, E. P., Cardarelli, C., Gottesman, M. M., Pastan, I., and Seamon, K. B. (1994) *Mol. Pharmacol. 46*, 329−337.
7. Greenberger, L. M., Lisanti, C. J., Silva, J. T., and Band Horwitz, S. (1991) *J. Biol. Chem. 266*, 20744−20751.
8. Bruggemann, E. P., Germann, U. A., Gottesman, M. M., and Pastan, I. (1989) *J. Biol. Chem. 264*, 15483−15488.
9. Loo, T. W., and Clarke, D. M. (1993) *J. Biol. Chem. 268*, 3143−3149.
10. Loo, T. W., and Clarke, D. M. (1994) *J. Biol. Chem. 26*, 7243−7248.
11. Loo, T. W., and Clarke, D. M. (1993) *J. Biol. Chem. 268*, 19965−19972.
12. Ramachandra, M., Ambudkar, S. V., Gottesman, M. M., Pastan, I., and Hrycyna, C. A. (1996) *Mol. Biol. Cell 7*, 1458−1498.
13. Hrycyna, C. A., Ramachandra, M., Pastan, I., and Gottesman, M. M. (1998) *Methods Enzymol. 292*, 456−473.
14. Current Protocols in Molecular Biology, 1997, (Ausubel et al., Ed.), J. Wiley, Inc., Boston.
15. Fuerst, T. R., Niles, E. G., Studier, F. W., and Moss, B. (1986) *Proc. Natl. Acad. Sci. 83*, 8122−8126.
16. Elroy-Stein, O., Fuerst, T., and Moss, B. (1989) *Proc Natl Acad Sci 86*, 6126−6130.
17. Higuchi, R. 1992 in *PCR Technology* (Ehrlich, H. A., Ed.), pp 61−70. W. H. Freeman and Company, New York.
18. Moss, B. (1991) *Science 252*, 1662−1667.
19. Germann, U. A., Chambers, T. C., Ambudkar, S. V., Licht, T., Cardarelli, C. O., Pastan, I., and Gottesman, M. M. (1996) *J. Biol. Chem. 271*, 1708−1716.
20. Bruggemann, E. P., Chaudhary, V., Gottesman, M. M., and Pastan, I. (1991) *BioTechniques 10*, 202−209.
21. Sarkadi, B., Price, E. M., Boucher, R. C., Germann, U. A., and Scarborough, G. A. (1992) *J. Biol. Chem. 267*, 4854−4858.
22. Urbatsch, I. L., Sankaran, B., Weber, J., and Senior, A. E. (1995) *J. Biol. Chem. 270*, 19383−19390.
23. Hanna, M., Brault, M., Kwan, T., Kast, C., Gros, P. (1996) *Biochemistry 35*, 3625−3635.
24. Loo, T. W., and Clarke, D. M. (1994) *Biochemistry 33*, 14049−14057.
25. Dey, S., Ramachandra, M., Pastan, I., Gottesman, M. M., and Ambudkar, S. V. (1997) *Proc. Natl. Acad. Sci. 94*, 10594−10599.
26. Chen, G., Duran, G. E., Steger, K. A., Lacayo, N. J., Jaffrezou, J. P., Dumontet, C., and Sikic, B. I. (1997) *J. Biol. Chem. 272*, 5974−5982.
27. Tang-Wai, D. F., Kajiji, S., DiCapua, F., de Graaf, D., Roninson, I., and Gros, P. (1995) *Biochemistry 34*, 32−395.

BI980871+